Optical properties of individual site-controlled Ge quantum dots

Cite as: Appl. Phys. Lett. **106**, 251904 (2015); https://doi.org/10.1063/1.4923188
Submitted: 30 April 2015 • Accepted: 17 June 2015 • Published Online: 25 June 2015

Martyna Grydlik, Moritz Brehm, Takeshi Tayagaki, et al.

Optical properties of individual site-controlled Ge quantum dots

Martyna Grydlik,[1,2,3,a)] Moritz Brehm,[1,2,a)] Takeshi Tayagaki,[4,5] Gregor Langer,[1] Oliver G. Schmidt,[2,3] and Friedrich Schäffler[1]
[1]*Institute of Semiconductor and Solid State Physics, Johannes Kepler University Linz, Altenbergerstrasse 69, 4040 Linz, Austria*
[2]*Institute for Integrative Nanosciences, IFW Dresden, Helmholtzstr. 20, Dresden 01069, Germany*
[3]*Center for Advancing Electronics Dresden, CfAED, TU Dresden, Germany*
[4]*Institute for Chemical Research, Kyoto University, Uji, Kyoto 611-0011, Japan*
[5]*Research Center for Photovoltaics, National Institute of Advanced Industrial Science and Technology, 1-1-1 Umezono, Tsukuba, Ibaraki 305-8568, Japan*

(Received 30 April 2015; accepted 17 June 2015; published online 25 June 2015)

We report photoluminescence (PL) experiments on individual SiGe quantum dots (QDs) that were epitaxially grown in a site-controlled fashion on pre-patterned Si(001) substrates. We demonstrate that the PL line-widths of single QDs decrease with excitation power to about 16 meV, a value that is much narrower than any of the previously reported PL signals in the SiGe/Si heterosystem. At low temperatures, the PL-intensity becomes limited by a 25 meV high potential-barrier between the QDs and the surrounding Ge wetting layer (WL). This barrier impedes QD filling from the WL which collects and traps most of the optically excited holes in this type-II heterosystem. [http://dx.doi.org/10.1063/1.4923188]

During the last years, the heteroepitaxial growth of Ge on Si has become a model system for the strain-driven self-assembly of quantum dots (QDs).[1–4] A main motivation for studying the optical properties of this material system is the prospect of efficient light emitters and single photon sources in the near infrared spectral range for monolithic integration into a silicon device platform.[5] Recent progress in site-controlled growth of SiGe QDs on pre-patterned Si(001) substrates,[6–10] and their commensurable embedding into photonic crystal slabs[11] has opened a unique route toward deterministic positioning of individual SiGe QDs in photonic crystal resonators. Yet, optical studies were mainly performed on ensembles of SiGe QDs, which cause broadening of the photoluminescence (PL) lines due to variations in QD size[12–16] and local composition.[17] Spectroscopy on single QDs appears to be a domain of III–V[18–20] and II–VI[21,22] heteromaterials, whereas optical measurements on isolated group-IV nanostructures were only reported for dispersed porous-Si grains[23] and Si pillars in an oxide matrix.[24,25]

Here, we study the optical properties of individual SiGe QDs. These have type-II band alignment, where holes are confined within the QDs, whereas electrons are located on the Si-side of the hetero-interface between QDs and Si matrix (lower inset in Fig. 3). In order to address single QDs, we used site-controlled self-assembly on pre-patterned Si(001) substrates to define SiGe QD arrays with several μm wide period.[8,26] These allow focusing of the PL detection spot onto a single QD. Moreover, the Ge distribution within the individual dots becomes more homogeneous,[17] which leads to narrower PL emission lines than if grown randomly on planar Si(001) substrates.[7,17] We also studied QD filling with holes from the surrounding Ge wetting layer (WL), which, for geometrical reasons, collects most of the optically generated holes.

The investigated SiGe QD-arrays were prepared in two steps. First, we fabricated on Si(001) float-zone substrates two-dimensionally (2D) periodic arrays of cylindrical pits by electron beam lithography and reactive ion etching. The pits have a diameter of ~200 nm, a depth of ~50 nm, and spacing of $d_{pit} = 3.4\ \mu$m. In the second step, the hetero-layers were grown by molecular beam epitaxy (MBE) in a Riber Siva 45 facility on these templates. The substrates were chemically pre-cleaned, and hydrogen passivated in 1% hydrofluoric acid[27] immediately before being introduced into the load-lock chamber. After *in-situ* degassing at 700 °C for 40 min, a 45 nm thick Si buffer layer was grown at a rate of 0.6 Å/s with the substrate temperature being ramped up from 450 °C to 550 °C. Hereafter, three monolayers (MLs) of Ge were deposited at 700 °C at a rate of 0.03 Å/s. Finally, a 30 nm thick Si cap was grown at 350 °C to avoid intermixing with the thin Ge WL and the Ge QDs.[28]

After growth, the surface of the samples was characterized *ex-situ* using a Digital Instruments Dimension 3100 atomic force microscope (AFM). Micro-PL measurements were carried out at sample temperatures (T_{PL}) ranging from 10 K to 80 K. PL was excited by a frequency doubled Nd:YVO_4 laser emitting at 532 nm, which was focused by an objective lens onto the sample with a spot diameter $< 2\ \mu$m. The detection spot had a diameter of $\approx 4\ \mu$m, as determined by a modified knife-edge method.[26] The PL signal was dispersed in a grating spectrometer and recorded with a liquid-nitrogen cooled InGaAs line detector.

An AFM micrograph of the investigated QD array is shown in the inset of Fig. 1. Dotted circles indicate the size of the detection spot,[26] revealing that only one or, at most, two QDs contribute to the PL signal. Figure 1 shows excitation-power dependent PL-signals from the Si-bulk, the

a)Electronic addresses: moritz.brehm@jku.at and martyna.grydlik@jku.at

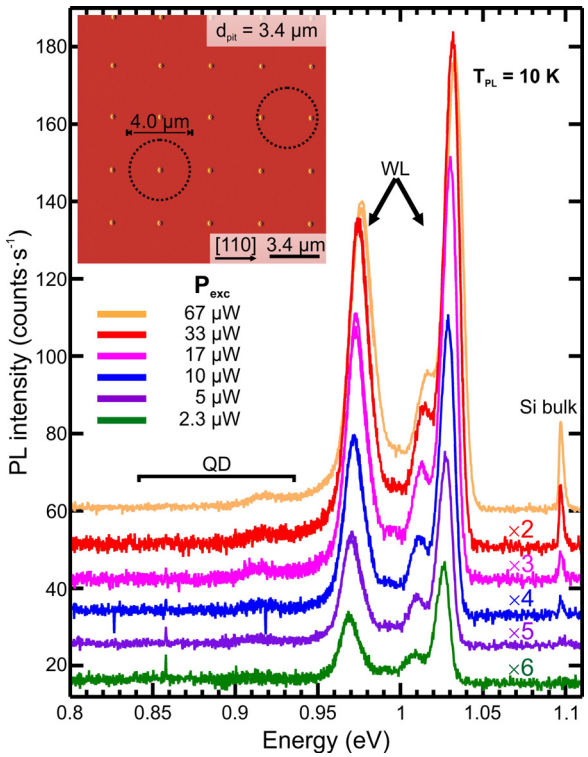

FIG. 1. P_{exc}-dependent PL spectra from individual QDs for $T_{PL} = 10$ K. The spectra are vertically shifted. P_{exc} was 67 μW (orange spectrum), 33 μW (red), 17 μW (pink), 10 μW (blue), 5 μW (violet), and 2.3 μW (green spectrum). In the inset, an AFM micrograph in derivative mode presents the field with $d_{pit} = 3.4$ μm. The dotted circles indicate the size of the detection spot.

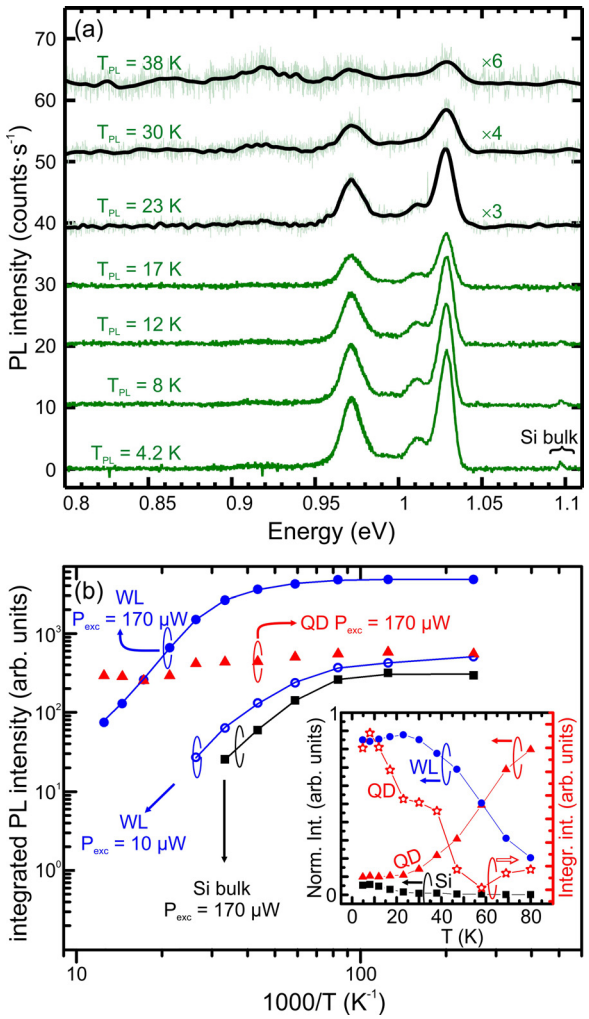

FIG. 2. (a) Temperature-dependence of PL-spectra from individual QDs at $P_{exc} = 10$ μW. The spectra are vertically shifted for reasons of visibility, and spectra obtained with $T_{PL} > 17$ K are magnified by a factor indicated in the figure. The black curves represent the smoothened spectra to guide the eye. (b) Integrated intensities for the Si bulk peak (black squares), the QDs (red triangles), and the WL (blue circles). The full symbols correspond to an excitation power of 170 μW, the open symbols to $P_{exc} = 10$ μW. The solid lines are fits from which the activation energies were determined. The inset in (b) shows a zoom-in of the integrated PL-intensity of the QDs (open star symbol) as well as the integrated PL-intensities of Si bulk, the WL and the QDs, normalized to the total PL-intensity for $P_{exc} = 170$ μW (full symbols).

WL and the QDs at $T_{PL} = 10$ K. The Si bulk signal appears at higher excitation powers near 1.1 eV as the transversal-optical-phonon (TO) replica of the Si bulk exciton. The WL related PL-signals appear between about 0.95 eV and 1.05 eV, with the most pronounced emission lines being the no-phonon (NP) line and a TO-phonon replica[29,30] at ~1.025 eV and ~0.97 eV, respectively. The QD emits between 0.8 eV and 0.95 eV, but the NP and TO lines cannot be resolved (see, e.g., green spectrum in Fig. 1, $P_{exc} = 2.3$ μW). Even for low excitation powers of $P_{exc} < 10$ μW, the WL signal dominates.

In Ref. 26, the existence of an activation energy barrier was discussed that prevents at low T_{PL} charge carriers bound to the WL to diffuse to the global potential minima in the QDs. To assess the involved activation energies, we performed temperature-dependent PL-spectroscopy with $P_{exc} = 10$ μW (Fig. 2(a)). The black guides to the eye represent smoothened spectra using a Savitzky-Golay-Filter.[31] Figure 2(b) shows on a double logarithmic scale the temperature-dependence of the integrated PL intensities from Si bulk, WL and QDs for an excitation power of 170 μW, as well as the PL-intensity of the WL for $P_{exc} = 10$ μW. The data were fitted according to Refs. 14 and 15

$$I_{WL}(T_{PL}) = I_0 \cdot (1 + A_1 \cdot \exp(-E_{A1}/k_B T_{PL}) + A_2 \cdot \exp(-E_{A2}/k_B T_{PL}))^{-1}, \quad (1)$$

where $I_{WL}(T_{PL})$ and I_0 and are the integrated WL PL-intensities at T_{PL} and at10 K, respectively, A_1 and A_2 are scaling coefficients, E_{A1} and E_{A2} are activation energies, and k_B is the Boltzmann constant. Two activation energies are required for a good fit. For the lower one, we found $E_{A1} \approx 5$ meV, which corresponds to the exciton binding energy of the type-II quantum-well potential of the WL.[32,33] The extracted value for E_{A2} was 25.4 ± 1.3 meV, which we attribute to hole transfer from the WL into the QDs over an energy barrier formed by a reduced WL thickness at the periphery of the dots.[34] We also considered an additional temperature-dependent term in Eq. (1), which should account for the different dimensionalities of the bound states in the WL and the QDs,[35] but found little influence on the two activation energies extracted from the simplified equation (1).[36]

The inset in Fig. 2(b) presents the integrated PL intensities from Si bulk, WL, and the QDs, normalized to the total PL intensity for $P_{exc} = 170$ μW. It is evident that thermal quenching of the WL-related PL signal is concomitant with a

transition of carriers into the QDs. A schematic illustration of the related carrier diffusion paths is shown in the upper inset of Fig. 3. We used the findings of Ref. 34 to determine the location of the activation barrier E_{A2}, i.e., the region where the WL becomes thinnest. Notice that for $d_{pit} = 3.4\,\mu m$, the projected surface of the QDs (5.55×10^3 nm^2) amounts to only about 0.05% of the total unit cell area (1.156×10^7 nm^2). Thus, almost all generated electron-hole pairs diffuse to the WL quantum well, where they become trapped because E_{A2} prevents diffusion into the QDs. Thus, for very low temperatures effective PL emission from the QDs is unlikely.

This finding is confirmed by the PL measurements in Fig. 3, which were carried out at $T_{PL} = 40$ K. In contrast to the 10 K-PL spectra in Fig. 1, where QD signals are barely detectable, some of the holes trapped in the WL can now overcome E_{A2} and diffuse into the QD. Simultaneously, the integrated PL signal decreases because of the low exciton binding energy E_{A1} and phonon-induced thermal quenching.[14] Overall, the relative contribution of carrier recombination in the QDs increases (inset in Fig. 2(b)) which leads to the observation of two QD-related peaks in the energy range between 0.83 and 0.95 eV (Fig. 2(a)).

To minimize line broadening by state-filling, we investigated the PL spectra of individual QDs at extremely low excitation powers between $0.1\,\mu W < P_{exc} < 1.4\,\mu W$. A series of spectra measured at $T_{PL} = 40$ K are displayed in Figure 4. When decreasing P_{exc} from about $30\,\mu W$ to $0.1\,\mu W$, we observed that the line-width of the QD-related NP-peak at 920 meV decreases to a full-width-at-half-maximum (FWHM) of about 16 meV, following the empirical power law $FWHM = A \cdot P_{exc}^{\ m}$ with $A = 0.02006$ and $m = 0.11025$. These widths are significantly sharper than PL lines from any SiGe QD ensembles published so far.[7,16] However, they are still, broader than the ones observed from top-down fabricated Si QDs,[25] and substantially broader than those of ordered InAs QDs,[20] even though we employed comparable excitation power densities.

The relatively broad single-QD PL signals even at low P_{exc} are caused by the interplay of several detrimental effects. (i) The indirect bandgap and the type-II band alignment in SiGe QDs lead to carrier lifetimes in the μs range[37,38] that are substantially longer than, e.g., in InAs

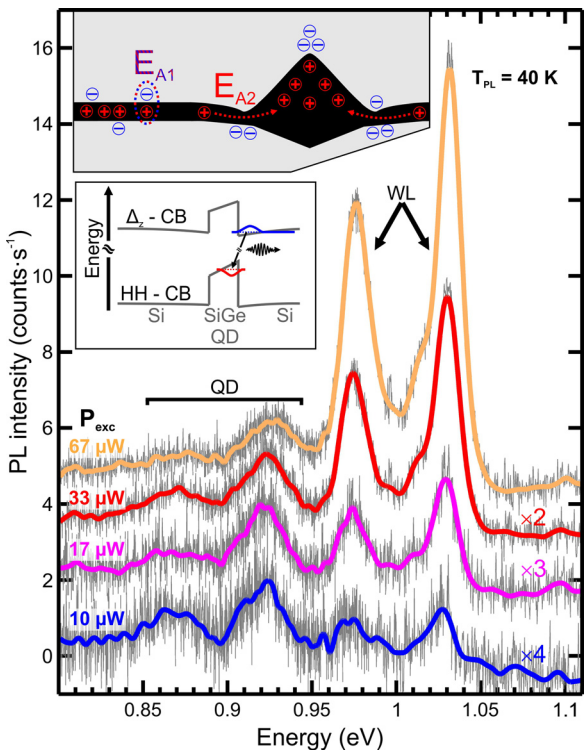

FIG. 3. P_{exc}-dependent PL spectra from individual QDs for $T_{PL} = 40$ K. The spectra are vertically shifted. The thick curves present smoothened spectra as guides for the eye. The upper inset schematically depicts a Ge QD in a pit (black) in a surrounding Si matrix (grey). Electrons and holes are depicted as "−" and "+," respectively. The locations of the experimentally determined activation barriers E_{A1} and E_{A2} are indicated. The lower inset shows the type-II band alignment of a SiGe QD. It is based on self-consistent calculations and the assumption of increasing Ge concentration in growth direction (left to right). The global conduction band minimum corresponds to the two-fold degenerate Si valleys Δ_z along the [001] growth direction.

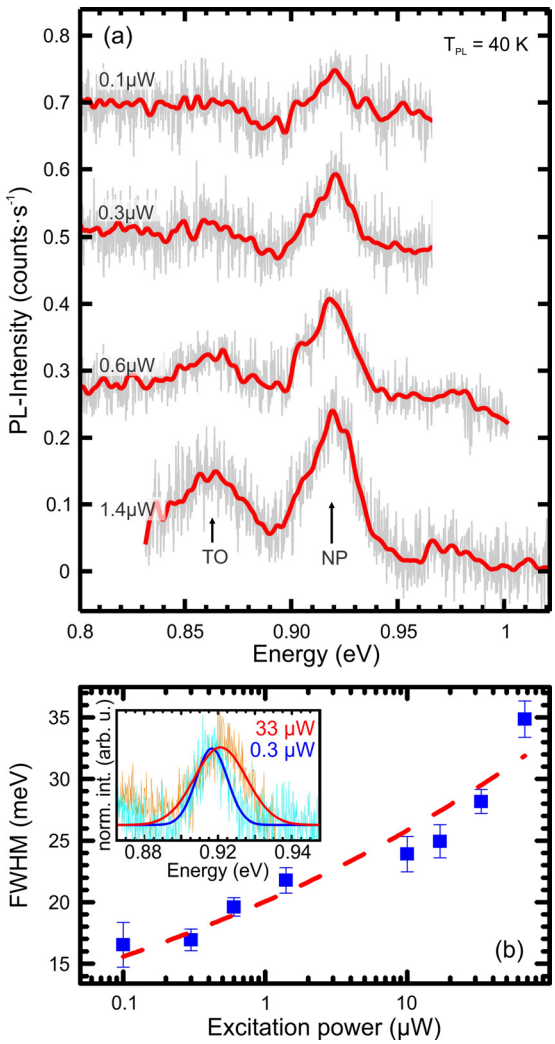

FIG. 4. (a) P_{exc}-dependent PL spectra from individual QDs for $T_{PL} = 40$ K. The excitation powers are indicated next to the spectra. The thick red curves present smoothened spectra and are only guides for the eye. The no-phonon (NP) signal at about 0.92 eV and the TO-phonon related peaks at about (0.865 eV) are indicated by arrows. (b) FWHM of the NP-QD-peak as a function of the excitation power. With decreasing power (from $67\,\mu W$ to $0.1\,\mu W$), the FWHM decreases by almost 20 meV. The red-dashed line presents a phenomenological power law fit using a Gaussian function. The inset shows the PL-QD NP peak with the corresponding Gaussian fits for $P_{exc} = 33\,\mu W$ and $0.3\,\mu W$.

QDs. Thus, even at our lowest P_{exc}, which is at the limits of experimental feasibility, filling effects are expected to be important. (ii) Level filling becomes in particular important in site-controlled SiGe QDs, because their rather homogeneous composition[17,39] causes spreading of the hole wave functions over most of the QD.[17] Consequently, the lowest ten hole levels have been estimated to be just ≈15 meV apart.[17] In addition, the strain distribution leads to a splitting of the six-fold degenerate conduction band of the Si matrix near the apex and the four base corners of the pyramidal-shaped QDs, where the electrons are located,[17,40] adding to the complex and dense system of energy levels. (iii) Another major contribution to line broadening in long-time averaged spectra comes from spectral diffusion[41,42] caused by charge fluctuations in the vicinity of the QDs. Such fluctuations can, for instance, be associated with growth defects, e.g., in the low-temperature Si cap layer. Moreover, thermally induced charge fluctuations of the weakly bound electrons of our type-II excitons (upper inset in Fig. 3) would lead to differently charged excitonic complexes.[43,44] Their energy shifts with respect to the neutral exciton level were predicted to be enhanced in type-II heterostructures.[45] (iv) Since the SiGe/Si heterosystem is indirect both in real and k-space, phonon broadening at T_{PL} is another expected contribution to the observed line width.

Two strategies appear feasible to further reduce the line widths of SiGe QDs. For one, lower growth temperatures could suppress interdiffusion and should thus allow smaller QDs with well separated hole confinement levels. Second, locating a single QD in a photonic crystal cavity[11] will lead to reduced radiative lifetimes due to the Purcell effect, which would also reduce level filling effects. Under these conditions, time resolved experiments should allow us to separate the aforementioned transition mechanism and to gain access to the intrinsic linewidths of individual transitions. Such forthcoming experiments will also be applied to recently developed SiGe QD light emitters,[46] which show greatly enhanced PL intensities even at room temperature, and might therefore be well suited for Si-based single photon sources.

In summary, we studied optical PL properties of site-controlled SiGe QD arrays with periods of 3.4 μm and demonstrated PL-emission from individual QDs. The related line-widths decrease with decreasing PL excitation power, reaching FWHW of 16 meV at low excitation densities. Power-dependent PL studies also highlight the role of an activation barrier, which has to be overcome by holes trapped in the WL to reach the global potential minima in the QDs.

This work was supported by the Austrian Science Funds (FWF) via Schrödinger Scholarship J3328-N19 and the Project Nos. F2502-N17 and F2512-N17 of SFB025: *IRON*. M.G. and O.G.S. acknowledge support from the Center for Advancing Electronics Dresden, CfAED. T.T. was supported by the ICR-KU International Short-term Exchange Program for Young Researchers. The authors thank T. Fromherz and F. Hackl for helpful discussions.

[1]J. Stangl, V. Holý, and G. Bauer, Rev. Mod. Phys. **76**, 725–783 (2004).
[2]J. J. Zhang, M. Brehm, M. Grydlik, and O. G. Schmidt, Chem. Soc. Rev. **44**, 26–39 (2015).
[3]J.-N. Aqua, I. Berbezier, L. Favre, T. Frisch, and A. Ronda, Phys. Rep. **522**, 59–189 (2013).
[4]S. Kiravittaya, A. Rastelli, and O. G. Schmidt, Rep. Prog. Phys. **72**, 046502–34 (2009).
[5]A. Alduino and M. Paniccia, Nat. Photonics **1**, 153 (2007).
[6]Z.-Y. Zhong, A. Halilovic, T. Fromherz, F. Schäffler, and G. Bauer, Appl. Phys. Lett. **82**, 4779–4781 (2003).
[7]C. Dais, G. Mussler, H. Sigg, E. Müller, H. H. Solak, and D. Grützmacher, J. Appl. Phys. **105**, 122405 (2009).
[8]M. Grydlik, G. Langer, T. Fromherz, F. Schäffler, and M. Brehm, Nanotechnology **24**, 105601 (2013).
[9]Y. J. Ma, Z. Zhong, Q. Lv, T. Zhou, X. J. Yang, Y. L. Fan, Y. Q. Wu, J. Zou, and Z. M. Jiang, Appl. Phys. Lett. **100**, 153113 (2012).
[10]C. J. Duska and J. A. Floro, J. Mater. Res. **29**, 2240–2249 (2014).
[11]R. Jannesari, M. Schatzl, F. Hackl, M. Glaser, K. Hingerl, T. Fromherz, and F. Schäffler, Opt. Express **22**, 25426–25435 (2014).
[12]P. Schittenhelm, M. Gail, and G. Abstreiter, J. Cryst. Growth **157**, 260–264 (1995).
[13]O. G. Schmidt, C. Lange, and K. Eberl, Appl. Phys. Lett. **75**, 1905–1907 (1999).
[14]J. Wan, Y. H. Luo, Z. M. Jiang, G. Jin, J. L. Liu, K. L. Wang, X. Z. Liao, and J. Zou, Appl. Phys. Lett. **79**, 1980 (2001).
[15]B. V. Kamenev, L. Tsybeskov, J.-M. Baribeau, and D. J. Lockwood, Appl. Phys. Lett. **84**, 1293–1295 (2004).
[16]M. V. Shaleev, A. V. Novikov, N. A. Baydakova, A. N. Yablonskiy, O. A. Kuznetsov, D. N. Lobanov, and Z. F. Krasilnik, Semiconductors **45**, 198–202 (2011).
[17]M. Brehm, M. Grydlik, F. Hackl, E. Lausecker, T. Fromherz, and G. Bauer, Nanoscale Res. Lett. **5**, 1868–1872 (2010).
[18]J. Y. Marzin, J. M. Gerard, A. Izrael, D. Barrier, and G. Bastard, Phys. Rev. Lett. **73**, 716–719 (1994).
[19]L. Landin, M. S. Miller, M.-E. Pistol, C. E. Pryor, and L. Samuelson, Science **280**, 262–264 (1998).
[20]P. Atkinson, S. Kiravittaya, M. Benyoucef, A. Rastelli, and O. G. Schmidt, Appl. Phys. Lett. **93**, 101908 (2008).
[21]A. Gustafsson, M.-E. Pistol, L. Montelius, and L. Samuelson, J. Appl. Phys. **84**, 1715–1775 (1998).
[22]G. Sallen, A. Tribu, T. Aichele, R. André, L. Besombes, C. Bougerol, S. Tatarenko, K. Kheng, and J. P. Poizat, Phys. Rev. B **80**, 085310 (2009).
[23]M. D. Mason, G. M. Credo, K. D. Weston, and S. K. Buratto, Phys. Rev. Lett. **80**, 5405–5408 (1998).
[24]J. Valenta, R. Juhasz, and J. Linnros, Appl. Phys. Lett. **80**, 1070–1072 (2002).
[25]I. Sychugov, A. Fucikova, F. Pevere, Z. Yang, J. G. C. Veinot, and J. Linnros, ACS Photonics **1**, 998–1005 (2014).
[26]M. Brehm, M. Grydlik, T. Tayagaki, G. Langer, F. Schäffler, and O. G. Schmidt, Nanotechnology **26**, 225202 (2015).
[27]H. Lichtenberger, M. Mühlberger, and F. Schäffler, Appl. Phys. Lett. **82**, 3650–3652 (2003).
[28]M. Brehm, M. Grydlik, H. Groiss, F. Hackl, F. Schäffler, T. Fromherz, and G. Bauer, J. Appl. Phys. **109**, 123505 (2011).
[29]J. C. Sturm, H. Manoharan, L. C. Lenchyshyn, M. L. W. Thewalt, N. L. Rowell, J.-P. Noël, and D. C. Houghton, Phys. Rev. Lett. **66**, 1362–1365 (1991).
[30]J. Weber and M. I. Alonso, Phys. Rev. B **40**, 5683 (1989).
[31]A. Savitzky and M. J. E. Golay, Anal. Chem. **36**, 1627 (1964).
[32]C. Penn, F. Schäffler, G. Bauer, and S. Glutsch, Phys. Rev. B **59**, 13314 (1999).
[33]Y.-H. Kuo and Y.-S. Li, Appl. Phys. Lett. **94**, 121101 (2009).
[34]J. J. Zhang, A. Rastelli, O. G. Schmidt, and G. Bauer, Semicond. Sci. Technol. **26**, 014028 (2011).
[35]M. Wachter, K. Thonke, R. Sauer, F. Schäffler, H.-J. Herzog, and E. Kasper, Thin Solid Films **222**, 10–14 (1992).
[36]See supplementary material at http://dx.doi.org/10.1063/1.4923188 for the determination of the activation energies considering the dimensionalities of the initial and final states in the nanostructures.
[37]S. Fukatsu, H. Sunamura, Y. Shiraki, and S. Komiyama, Appl. Phys. Lett. **71**, 258 (1997).
[38]B. V. Kamenev, L. Tsybeskov, J.-M. Baribeau, and D. J. Lockwood, Phys. Rev. B **72**, 193306 (2005).
[39]T. U. Schülli, G. Vastola, M.-I. Richard, A. Malachias, G. Renaud, F. Uhlík, F. Montalenti, G. Chen, L. Miglio, F. Schäffler, and G. Bauer, Phys. Rev. Lett. **102**, 025502 (2009).
[40]M. Brehm, T. Suzuki, T. Fromherz, Z. Zhong, N. Hrauda, F. Hackl, J. Stangl, F. Schäffler, and G. Bauer, New J. Phys. **11**, 063021 (2009).

[41]V. Türck, S. Rodt, O. Stier, R. Heitz, R. Engelhardt, U. W. Pohl, and D. Bimberg, Phys. Rev. B **61**, 9944 (2000).
[42]S. A. Empedocles and M. G. Bawendi, Science **278**, 2114 (1997).
[43]D. Gammon, E. S. Snow, B. V. Shanabrook, D. S. Katzer, and D. Park, Science **273**, 87 (1996).
[44]B. Patton, W. Langbein, and U. Woggon, Phys. Rev. B **68**, 125316 (2003).
[45]Ph. Lelong, K. Suzuki, G. Bastard, H. Sakaki, and Y. Arakawa, Physica E **7**, 393 (2000).
[46]M. Grydlik, F. Hackl, H. Groiss, M. Glaser, A. Halilovic, T. Fromherz, W. Jantsch, F. Schäffler, and M. Brehm, e-print arXiv:1505.03380.